Refereed Proceedings

The 12th International Conference on Fluidization - New Horizons in Fluidization Engineering

Engineering Conferences International *Year* 2007

Transient Characterization of Type B Particles in a Transport Riser

Lawrence J. Shadle* Esmail R. Monazam†

Joseph S. Mei‡

*National Energy Technology Laboratory, lshadl@netl.doe.gov

†REM Engineering Services PLLC

‡National Energy Technology Laboratory

TRANSIENT CHARACTERIZATION OF TYPE B PARTICLES IN A CIRCULATING FLUIDIZED BED RISER

Lawrence J. Shadle, Esmail R. Monazam*, and Joseph S. Mei
National Energy Technology Laboratory, U. S. Department of Energy
*REM Engineering Services PLLC, 3610 Collins Ferry Road
Morgantown, West Virginia 26507-0880

ABSTRACT

Simple and rapid dynamic tests were used to evaluate fluid dynamic behavior of granular materials in the transport regime. Particles with densities ranging from 189 to 2,500 kg/m^3 and Sauter mean size from 61 to 812 □m were tested in a 0.305 m diameter, 15.5 m height circulating fluidized bed (CFB) riser. The riser emptying time was linearly related to the Froude number in each of three operating regimes. The flow structure along the height of the riser followed a distinct pattern as tracked through differential pressures. These results are discussed to better understand the transformations that take place when operating over various regimes. The effects of pressure, particle size, and density on test performance are also presented.

INTRODUCTION

While there is a rich literature characterizing fluid dynamics of individual particles in gas flows (1), and to a lesser extent, densely loaded fluid beds (2,3) there is less information available on densely loaded gas-solids flow (4,5). In this regime the flow structure can be dominated by boundary conditions such as walls and end effects which necessitate large test units which are more expensive to build and operate. As a result the data available on the behavior of multiple sizes and densities in this regime is less common. A relatively rapid means of characterizing a given bed material was needed to facilitate filling this data gap.

In studying the character of mono-dispersed materials in densely loaded transport risers it is important to first understand when the system has transitioned from slugging (turbulent) to fast fluidization, and then to dense and dilute transport. Several researchers have summarized these transitions (6,7,8) providing correlations which allow us to estimate the solids and gas flows and properties required for the principal transitions. However, the transitions using the ΔP-G_s-U_g maps (9,10) are time consuming to measure leading to the development of several transient techniques (11,12). Monazam et al.(13,14) found that these methods can lead to ambiguous results due to observation of several transitions depending on the range of flow conditions tested. The riser size and CFB inventory may also influence the upper transition velocity that Bi and Grace (6) referred to as the transition to core-annular regime designated, V_{ca}. Monazam and Shadle (13) demonstrated that the ΔP-G_s-U_g plot could be recreated in a series of transient tests that were statistically indistinguishable from the steady state performance over much of the fast fluidization regime. They went on to show that in a given riser the transitions from slugging to fast fluidization bed (FFB), as well as the transition from FFB to core

The 12th International Conference on Fluidization - New Horizons in Fluidization Engineering, Art. 14 [2007]

annular (CA) or dilute flow could be clearly identified using these solids cutoff transients (14). In general, in these transient tests the slowest solids emptying times were observed at low flows below the classical choking velocity. Intermediate decay rates were found in the fast fluidized regime characterized by an S-shaped axial pressure profile with a denser solids fraction in the bottom of the riser. While the shortest solids emptying times were found at velocities above fast fluidization in which the riser was more homogenous in the axial direction. In this more homogeneous region the axial riser solids distribution were either uniform or C-shaped with denser regions near the bottom or top of the riser. The radial profiles exhibited either classical turbulent pattern or core annular flow pattern (15).

In this paper several materials were characterized using a protocol being developed at the National Energy Technology Laboratory. The transient method is further explored to better understand the effects of test conditions and test procedures modifications required for different particles. Limitations in the procedures are presented. The riser flow structure during transient tests is discussed to provide a better understanding of the transitions through different transport flow regimes.

EXPERIMENTAL

The riser is 0.305 m diameter and 15.45 m tall cylindrical vessel and has been operated with various non-mechanical valves all entering through 0.23 m diameter port at 0.27 m above a distributor plate. Details can be found elsewhere for test campaigns using glass beads (5,16), coke (17), and cork (18). Riser velocities were corrected for temperature and pressure as measured at the base of the riser. The mass circulation rate was continuously recorded by measuring the rotational speed of a twisted spiral vane located in the packed bed region of the standpipe (19). Steam was introduced into the air supply header as needed to control the relative humidity between 20 and 50%. A total of twenty incremental differential pressures were measured across the length of the riser. The uncertainty for the total riser pressure drop was ± 0.45 Pa/m at 95% CL. Apparent solids holdup was estimated from the measured differential pressures.

Table 1. Granular material physical and fluid dynamic properties

	glass beads		coke	cork
d_p, μm	61	180	230	812
ρ_s, kg/m^3	2426	2483	1710	189
U_{mf}, m/s	0.86	3.17	2.35	15.59
V_{CC}, m/s	1.84	2.11	--	--
V_{CA}, m/s	2.96	4.57	5.79	3.33

The characterization of each bed material is also presented in Table 1. They all behaved like type B materials. The particle density was measured by water displacement in a pycnometer. The mean particle size was taken from a sieve analysis. The minimum fluidization velocity was taken by stepwise increasing aeration velocity in a 2.5 cm diameter fluid bed with a metal porous plate distributor. The values of V_{CC} and V_{CA} were determined by solids cutoff experiments at the appropriate gas velocities as described below.

RESULTS AND DISCUSSION

Simple and rapid dynamic tests were used to evaluate the dynamic response of 61 and 180 μm glass beads, by simply and abruptly halting the solids flow in the middle of a steady state operation. This was accomplished by stopping the standpipe and L-valve aeration and, when necessary, evacuating the trapped compressed gas held within packed solids at the base of the standpipe. These tests were conducted for superficial gas velocities from 1.3 to 7.3 m/s.

Changes in Flow Structure through Regime Transitions

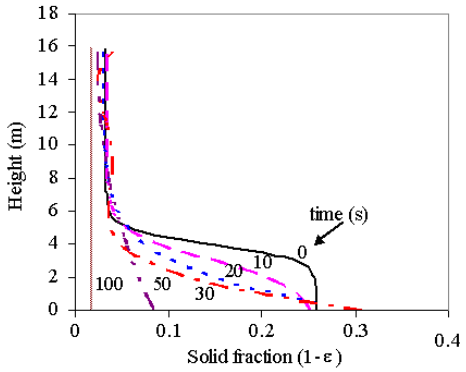

Figure 1. Axial solids fraction profile after initiating the solids cutoff transient at U_g=2.14 m/s for 61 μm glass beads.

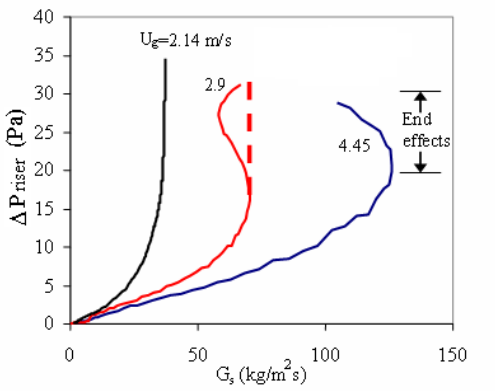

Figure 2. Translated ΔP-Gs-Ug flow regime map from transients for 61 μm glass beads.

The transients for 61 μm glass beads are presented in Figures 1 through 4. Using the methodology described earlier (13) the ΔP-G_s-U_g plot was generated from the solid cutoff transients (Figure 1). The middle curve for 2.9 m/s exhibited distinct curvature which was observed in the earlier study but left unexplained because it represented only a minor distortion within the entire range of solids flux conditions tested with cork. However, it was reproducibly observed. In the higher flow case a slightly different distortion was found. During the transient the data points start at the highest ΔP and systematically drop with time. According to the procedure the solids flux, G_s, is taken from the derivative of the ΔP with respect to time. In the lowest flow case the G_s matched the saturated carrying capacity (SCC). This is found in all cases in which the dense lower region does not reach the top of the riser and is the basis for the SCC method developed by Monazam et al. (20). For the 2.14 m/s flow case the estimated G_s dropped and then recovered with both the initial and peak flux matching the SCC and steady state flux reasonably well. By contrast, in the more dilute, high gas flow case, the G_s started out lower than the steady state value and gradually increased until the values almost matched.

The distortions in the translated ΔP-G_s-U_g plot can be better understood by looking at the differential pressures through the transient. For example, the axial pressure profiles during the transient taken at 2.14 m/s are shown in Figure 1. These were prepared by fitting the instantaneous differential pressure drops along the riser with a 5th degree polynomial. The apparent solids holdup was determined from these pressure drops assuming no contribution from acceleration and gas-solids friction. This steady state test condition was clearly S-shaped indicating that the unit was operating in the FFB regime as evidenced by the high solids fraction near the bottom and low solids fraction at the top (t_d = 0 s). The solids fraction in the bottom of the riser decreased first, while the upper region of the riser remained unchanged. Not until the bottom of the riser reached the same solids concentration as that in the upper region did the concentration throughout begin to decay. This confirms the observations reported earlier over the entire FFB regime for cork (13). The axial profiles at 2.9 and 4.45 m/s did not produce such clearly identifiable dense bed as found in Figure 1.

More detailed analysis of the differential ΔP's at various axial positions are presented in Figure 3 for the high flow CA case and in for the low flow case in Figure 4 for the FFB flow regime. In the CA case the pressure transducer at the base of the riser (0.6 m) recorded a rapidly decaying signal immediately after the solids cutoff. The transducers immediately above the acceleration zone recorded an increased apparent solids hold-up only seconds later peaking between 10 and 30 seconds.

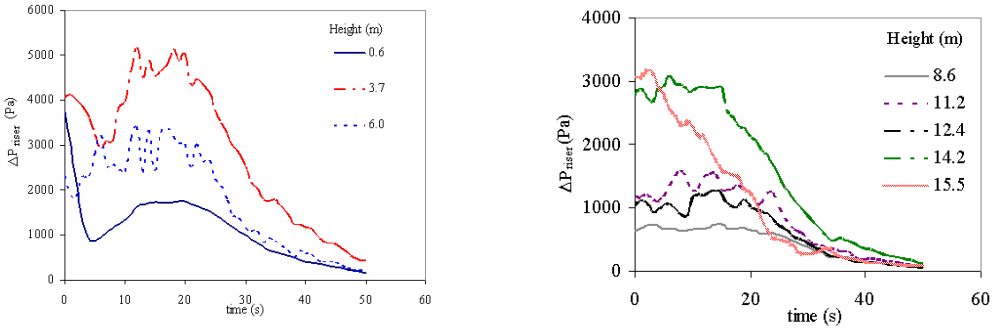

Figure 3. Differential pressure drops along the riser for CA regime: U_g =4.45 m/s and 61 μm glass beads.

These can be thought of as waves of solids surging towards the exit as part of the overall emptying process. The transducer at the top of the riser, 15.5 m (Figure 3), displayed a reduction in the apparent solids holdup immediately after the acceleration zone was depleted (~10 seconds). This depletion of the dense region at the very top of the riser continued for the next 10 to 15 seconds before any of the other pressure measurements began to decrease. This represented a depletion of the inverted dense bed at the top of the riser. The inverted dense bed is a build up of solids resulting from the abrupt exit that causes solids to back-mix or reflux into the regions immediately below (5). The next region to record a decreased pressure was the next highest transducer at 14.2 m. By the time the inverted dense bed at 14.2 m was depleted, the very top of the riser had reached the same apparent bed density as the middle of the riser. Concurrently, the solids hold-up at the very bottom of the riser began to steadily decrease. By thirty seconds after the solids cutoff, the solids densities were similar in all of the riser sections and they were all decreasing at the same rate. These changes in the solids profile in time after the cutoff were found to display the same trends as those changes in the steady-state solids profile observed with solids flux. As the solids flux increased, the solids holdup increased uniformly until denser regions developed at both top and bottom of the riser, then the solids hold-up increased in these end regions with further increased solids flux. Also, the G_s (estimated from rate of change in riser □P over the solids cutoff) was found to be most accurate in the CA and dilute regimes.

In the FFB regime the changes in apparent solids fraction profile along the riser change in quite a different manner. Unlike the higher flow, CA regime, no initial decrease was observed in the apparent solids holdup in either the very top or very bottom of the riser (Figure 4). Instead, the pressure decay began at a region in the riser corresponding to the top of the dense bed at 3.7 m. The dense bed was gradually expelled moving sequentially lower into the riser until, by 80 s after the solids cutoff, the entire bed reached a more uniform concentration of solids. Beyond this point all of the pressure transducers recorded comparable decreases in apparent solids levels, suggesting a more uniform depletion of solids much like what occurred at the end of the higher flow case. These changes were also found to

resemble those that occur in the riser as the solids flux was reduced through the FFB regime. In the FFB regime the solids fractions in both the upper and lower portions of the riser are known to be independent of solids flux and only the height of the dense bed decreases with decreasing solids flux. Once the solids flux drops below the SCC, then the solids fraction decreases and that decrease is uniformly distributed across the length of the riser. Thus, when interpreting the cases intermediate between FFB and CA regimes in the transient ΔP-G_s-U_g plot (Figure 1), the distortion at the top can be thought to be a result of incompletely developed dense bed and competing depletion of the end regions. For clarity a dashed line indicative of the SCC has been incorporated on this curve representing a more realistic estimate of the corresponding G_s.

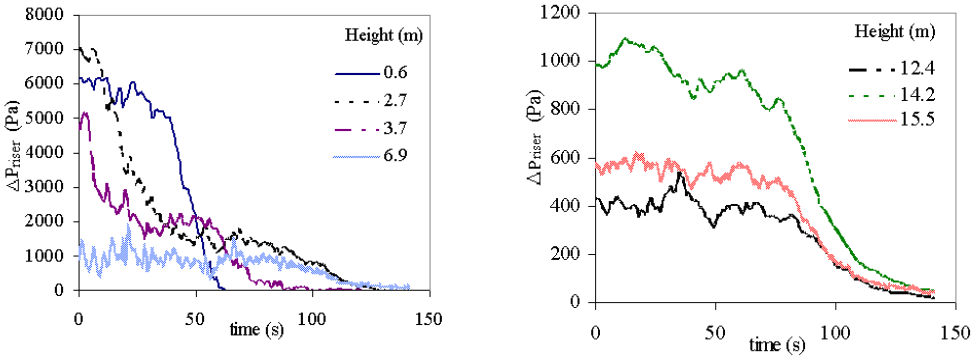

Figure 4. Differential pressure drops along the riser for the FFB regime: U_g=2.14 m/s and 61 μm glass beads.

Transient Cutoff Test Method

Tests were conducted with 180 □m glass beads to identify the critical transitions in operating regime for this new bed material. In addition, a factorial test was designed to determine whether the regime transitions as measured using solids cutoff transients are defined by the relative mass flows of solids and gases or upon the relative velocities. In pneumatic conveying the solids load limit is generally stipulated by the relative mass of gases and solids, while the drag coefficient is a function of the relative velocities. The tests were conducted over 8 levels evenly spaced with respect to the riser flow, F_t. The flow conditions were run in random order. The independent parameters were riser flow and gas pressure at the base of the riser (Table 2). The test matrix was a simple factorial design and duplicates tests were conducted to estimate the error. In addition the inventory in the riser was controlled by maintaining a constant standpipe height, H_{sp}. This was accomplished by adjusting the standpipe aeration, $F_{m,}$ in order to maintain the same steady state standpipe bed height for each different series of riser flows and pressures. In these tests the temperatures were controlled to 21 ± 0.33 C, Relative Humidity to 40 ± 0.4%, and steady state standpipe bed height to 7.0 ± 0.18 m (ranges from 95% confidence limits). Standpipe aeration was ramped to obtain maximum solids loading in the riser. After a steady state period the solids flow was abruptly halted leading to a dynamic, riser-pressure decay.

A summary of these factorial tests including the solids cutoff transients and prior steady state period is presented in Table 2. The results are grouped in pairs of duplicates which can be inspected to evaluate the repeatability. It can be seen that those duplicate pairs that had the largest differences between circulation rates or riser pressure drops were also the tests which exhibited the largest deviation from

The 12th International Conference on Fluidization - New Horizons in Fluidization Engineering, Art. 14 [2007]

the set-point especially with respect to the pressure at the base of the riser. This was the more difficult variable to control because it is a combination of the riser pressure drop as well as the action of a back pressure control valve at the outlet of the secondary cyclone.

Table 2. Results of 2^2 factorial scoping tests on the effect of pressure on decay times.

Test No.	Independent variables		Control variables			Dependent variables		
	F_t (m^3/hr)	P_b (bar)	H_{sp} (m)	F_m (m^3/hr)	U_g (m/s)	ΔP_r (bar)	M_s (lkg/hr)	t_d (sec)
SCG28	1559	0.619	7.32	9.6	3.90	0.556	18194	143
SCG21	1590	0.628	7.07	10.7	3.89	0.577	19736	144
SCG24	2271	0.646	7.68	20.4	5.53	0.530	64674	64
SCG27	2261	0.682	7.38	22.0	5.38	0.556	65434	60
SCG23	2294	1.088	7.01	16.3	4.39	0.519	26754	110
SCG26	2276	1.101	7.23	18.3	4.34	0.558	32182	104
SCG25	1561	1.099	7.01	11.1	3.00	0.510	9202	293
SCG22	1590	1.103	7.07	10.8	2.99	0.504	9961	274

A statistical analysis was conducted to evaluate the significance of the gas pressure or density on the emptying time during the solids cutoff transient. Each of the three factors tested (F_t, P_b, and F_t*P_b) was found to be significant at the 95% confidence limit using a standard F-test. Thus, the emptying time was shown to be influenced by more than just the mass flow of gas, and it also depended on the gas density or velocity. This might have been anticipated based on the relationship between the solids hold-up and the slip factor or relative gas-solids velocity. The general linear model was successful in explaining better than 99% of the variance in the test data. This could be equally well fit using a quadratic relationship with gas velocity. When this pressure test data was added to the regime transition plot using superficial gas velocities, considerable scatter was observed. Much of the deviations from the lines representing three regimes are eliminated by plotting the decay times against the Froude number. There still remained deviation within the fast fluid bed regime (FFB) as indicated by the scatter in emptying times for 180 micron glass beads near a Fr of 5000 in Figure 5 represented by the blue open squares. While this helped to separate the regimes it is not expected that this will adequately capture the effect of higher gas density or gas pressure. Additional analysis will be required to account for this pressure effect.

Transport Regimes of Various Granular Materials

The results of transient experiments are summarized in Figure 5 and tabulated in Table 1. As expected the glass beads of larger size had higher FFB-CA transition Froude No. and V_{ca} than the smaller beads. However, the slugging-FFB transition was different. The

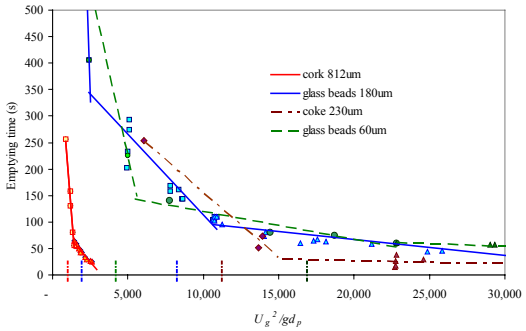

Figure 5. Transient decay curve for various bed materials displaying fitted lines as well as associated data points for each regime measured.

Froude No. for the slugging-FFB transition was lower for the larger beads due to the inverse dependence on particle size, while the V_{CC} was about 15% higher than that of the smaller beads. By contrast the FFB-CA transition, V_{CA}, was 50% higher for the larger beads. This confirmed that the two regime transitions involved different physical phenomena. Li (21) discuss these differences in terms of differences between particle fluid compromising and fluid dominated flow regimes.

The lowest density bed material exhibited the lowest FFB-CA transition Froude No. due to the fact that this material had the largest particle diameter. The associated V_{ca} for cork was somewhat higher than that for the smallest granular glass particle. It is also interesting to note that coke exhibited the highest V_{ca} and FFB-CA Froude No. transition even though it was intermediate in both size and density.

Particle Size Changes During Transients

During the solids flow cutoff transient the particle size distribution was measured along the centerline of the riser at an axial location 42' above the solids entry. The gas solids mixture was passed through an optical cell designed to gather forward scattered light from an incident laser beam using an Ensemble Particle Concentration System manufactured by TSI Inc. The resulting diffraction pattern was used to extract particle size distribution continuously. No attempt was made to isokinetically sample the fluid stream. The sample extraction rate was limited to less than 2.8 m^3/hr, thus making it less than 0.2% of the total flow stream. Typical results from these measurements are presented in Figure 6. This represents a volumetric percentage of the particles and is therefore skewed to preferentially reflect the concentrations of larger particles.

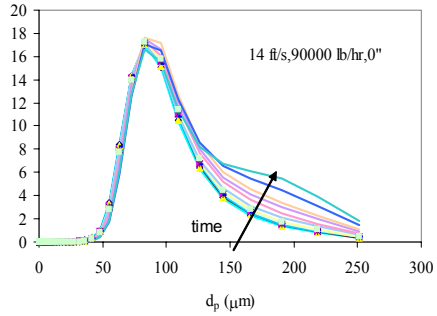

Figure 6. Particle size distribution in the riser as a function of time after the solids cutoff transient.

The size distribution of the particles remained constant over most of the transient; however, towards the end of the transient the particles remaining in the riser were found to be somewhat depleted of smaller size and enriched in larger particles. This was not unexpected and helped to identify the region of the transient relevant to characterizing the flow structure for the original granular feed. These limitations are expected to be dependent on the range over which the size distribution varies.

SUMMARY

Simple and rapid dynamic tests were used to evaluate the dynamics of granular materials with densities ranging from 189 to 2,500 kg/m^3 and mean sizes from 61 to 812 μm. Standpipe aeration was ramped to obtain maximum solids loading in the riser. The solids flow was then abruptly halted leading to a riser pressure decay. The associated solids flow rate was estimated for each time step from the changes in the pressure drop per unit time during riser emptying transient. Limitations for accurately estimating the related steady state condition were identified in each operating regime. Experimental methods required to obtain accurate unbiased results are discussed including effects of bed materials, gas pressure, and particle size distribution.

The 12th International Conference on Fluidization - New Horizons in Fluidization Engineering, Art. 14 [2007]

NOTATION

CA Core-Annular regime
d_p, Particle diameter, μm
FFB Fast Fluid Bed regime
F_m Standpipe aeration volumetric flow, m^3/hr
Fr Froude number, U_g^2/gd_p
F_t Total riser flow, m^3/hr
g gravitational constant
G_s Solids Flux, kg/m^2-s
H_{sp} Height of the standpipe bed, m
M_s Solids mass circulation rate, kg/hr
P_b Pressure at the base of the riser, bar
t_d Time for complete decay of riser pressure after a solids cutoff, sec.
U_{mf} Minimum fluidization velocity, cm/s
U_g Superficial gas velocity, m/s
V_{cc} Velocity marking the transition between FFB and CA regimes, m/s
V_{ca} Velocity marking the transition between FFB and slugging regimes, m/s
ρ_s Particle density, kg/m^3
ΔP Pressure drop across a length interval, Pa
ΔP_{riser} Pressure drop across the riser, Pa

REFERENCES

1 J.F. Davidson and D. Harrison, Fluidized Particles, Cambridge University Press, London, 1963
2 D. Kunii and O. Levenspiel, Fluidization Engineering, John Wiley & Sons, New York, 1984.
3 F.A. Zenz and D.F. Othmer, Fluidization and Fluid-Particle Systems, Reinhold Publishing Corp, New York, 1960.
4 Kim, S. W., Kirbas, G., Bi, H. T., Lim, C. J., Grace, J. R., 2004, Chemical Engineering Science, Vol. 59, pp. 3955
5 Joseph S. Mei, Lawrence J. Shadle, Paul C. Yue, Esmail R. Monazam, 2006, 12th International Fluidization Conference.
6 H. T. Bi, J. R. Grace, International Journal of Multiphase Flow, 21 (1995), 1229.
7 K. Smolders, J. Baeyens, Powder Technol., 119 (2001), 269.
8 H. T. Bi, L.-S. Fan, AIChE Annual Meeting, Los Angeles, November. 1991, p.17,
9 J. Yerushalmi, N.T. Cankurt, Powder Technol., 24 (1979) 187
10 Y.C. Li and M. Kwauk, In Fluidization; Grace, J.R., Matsen J.M., Eds, Plenum Press: New York, 1980, 537
11 J. F. Perales, T. Coll, M. F. Llop, L. Puigjaner, J. Arnaldos, J. Cassal, in: P. Basu, M. Horio, M. Hasatani (Eds.) Circulating Fluidized Bed Technology III, Pergamon , Oxford, 1990, p. 73.
12 D. Bai, A.S. Issangya, and J.R.Grace, Powder Technol., 97(1998), 59.
13 E.R. Monazam and L.J. Shadle, (2004), *Powder Technology,* 139 (2004) 89-97
14 E.R. Monazam, L.J. Shadle, J. Mei, and J. Spenik,(2005), *Powder Technology, 155(1), 17*
15 S.M. Seachman, P.C. Yue, E.M. Taylor, and L.J. Shadle (2005), AIChE Annual Meeting, Cincinnati, OH, Session 03006 Circulating Fluidized Beds, MS# 32940, pp.10
16 J. Mei, L.J. Shadle, E.R. Monazam, (2004), *11th International Fluidization,* Ischia, Italy, p. 411-418.
17 L. J. Shadle, J. Spenik, A. Sarra, and J. Ontko (2004), Ind. Eng. Chem. Research, 43(15), 4166-4173.
18 L. J. Shadle, E. R. Monazam, and J. S. Mei (2002), in: J. R. Grace, J. Zhu, H. de Lasa (Ed.), Circulating Fluidized Bed Technology VII, Canadian Society of Chemical Engineering, Ottawa, Canada, 2002, p. 255
19 J. C. Ludlow, L. Lawson, L. Shadle, M. Syamlal, in: J. R. Grace, J. Zhu, H. de Lasa (Ed.), Circulating Fluidized Bed Technology VII, Ottawa, Canada, 2002, p. 513.
20 E. R. Monazam, L. J. Shadle, and L. O. Lawson (2001), *Powder Technology*, 121, pp.205-212.
21 J. Li, Modeling, in Fast Fluidization, M. Kwauk Eds., Academic Press, 1994, 147.